Properties of spin-1/2 heavy baryons at nonzero temperature

A. Türkan,[1] G. Bozkır,[2] and K. Azizi[3,4,*]

[1]*Özyeğin University, Department of Natural and Mathematical Sciences, Çekmeköy, 34794 Istanbul, Turkey*
[2]*National Defense University, Army NCO Vocational HE School, Department of Basic Sciences, Altıeylül, 10185 Balıkesir, Turkey*
[3]*University of Tehran, Department of Physics, North Karegar Avenue, Tehran 14395-547, Iran*
[4]*Doğuş University, Department of Physics, Acıbadem-Kadıköy, 34722 Istanbul, Turkey*

(Received 12 July 2021; accepted 25 October 2021; published 18 November 2021)

The spectroscopic properties of single heavy spin-1/2 Λ_Q, Σ_Q, $\Xi_Q^{(\prime)}$, and Ω_Q baryons are investigated at finite temperature in the framework of the thermal QCD sum rule. We discuss the behavior of the mass and residue of these baryons with respect to temperature, taking into account contributions of nonperturbative operators up to dimension eight. We include additional operators coming from the Wilson expansion due to breaking the Lorentz invariance at nonzero temperature. The obtained results show that the mass of these baryons remain stable up to roughly $T = 108$ MeV while their residue is unchanged up to $T = 93$ MeV. After these points, the mass and residue start to diminish by increasing the temperature. The shifts in the mass and residue for both the bottom and charm channels are considerably large and we observe the melting of these baryons near to the pseudocritical temperature determined by recent lattice QCD calculations. We present our results for the mass of these baryons with both the positive and negative parity at the $T \to 0$ limit, which are consistent with the existing theoretical predictions as well as experimental data.

DOI: 10.1103/PhysRevD.104.094029

I. INTRODUCTION

One of the most attractive subjects in particle physics is to investigate the spectroscopic properties of hadrons at finite temperatures. Such studies provide us with a better understanding of the perturbative and nonperturbative natures of QCD at hot mediums. They will also help us in analyses of data provided by future heavy ion collision experiments aiming to investigate the hadronic properties and possible phase transitions to quark-gluon plasma (QGP) at finite temperatures and densities. In the last two decades, there have been significant experimental and theoretical studies on single heavy baryons in vacuum. Roughly all single heavy baryons containing a heavy b or c quark have been successfully observed [1]. The investigation of these baryons at a medium with nonzero temperature is a very prominent research subject now and it will be in the agenda of different experimental and theoretical studies.

*Corresponding author.
kazem.azizi@ut.ac.ir

Single heavy baryons (Qq_1q_2) are composite particles made of one heavy ($Q = b$ or c) and two light quarks ($q_{1,2} = u$, d, or s). These particles belong to either the antitriplet of the flavor antisymmetric state $\bar{\mathbf{3}}$ or the sextet of the flavor symmetric state 6. It is well known that total spin-parity of the ground state single heavy baryons in the sextet state is either $J^P = \frac{1}{2}^+$ or $J^P = \frac{3}{2}^+$ while spin-parity of the single heavy baryons in the antitriplet state is only $J^P = \frac{1}{2}^+$. In this paper, we study the spectroscopic parameters of the spin-1/2 heavy bottom/charmed baryons both in antitriplet and sextet representations, whose members are shown in Table I.

In the literature, a lot of theoretical studies on the investigation of the spin-1/2 heavy baryons in vacuum have been performed using different phenomenological approaches, such as the quark model [2,3], quark potential model [4], heavy quark effective theory [5–7], chiral perturbation theory [8], Feynman-Hellman theorem [9], the hypercentral approach [10–13], lattice QCD simulation [14–17], the relativistic (constituent) quark model [18–25], the chiral quark-soliton model [26], symmetry-preserving treatment of a vector × vector contact interaction model [27], QCD sum rules [28–39], etc. As we also previously mentioned, to better understand the hot and dense QCD matter created in relativistic heavy ion collision experiments, such as the Relativistic Heavy Ion Collider at

Brookhaven National Laboratory and the Large Hadron Collider (LHC) at the European Organization for Nuclear Research (CERN), the investigation of effects of temperature on spectroscopic properties of hadrons at nonzero temperature is needed. Such investigations can also help us to improve our understanding of phase transition, quark-gluon deconfinement, and chiral symmetry restoration. By increasing the temperature, a transition or chiral crossover [40,41] from the hadronic phase to the QGP phase may occur. Lattice QCD calculations show that the pseudocritical temperature is $T_{pc} \approx 155$ MeV for a chiral crossover [42,43] to QGP.

One of the most applicable and powerful phenomenological tools that can be used to analyze the spectroscopic properties of hadrons at nonzero temperature is the thermal QCD sum rule method (TQCDSR). This method is the thermal version [44] of the QCD sum rule, firstly introduced by Shifman, Vainshtein, and Zakharov for mesons at zero temperature [45] and then applied to baryons in vacuum by Ioffe [46]. In the thermal version, some additional operators appear in the operator product expansion (OPE/Wilson expansion) due to the breaking of the Lorentz invariance and vacuum expectation values are replaced by their thermal forms at finite temperature. The essential objective of this study is to extend our previous work on the thermal properties of the spin-3/2 heavy baryons at nonzero temperature [47] and investigate the shifts on the mass and residue of the spin-1/2 heavy Λ_Q, Ξ_Q, Σ_Q, Ξ'_Q, and Ω_Q baryons with respect to temperature using the TQCDSR method. In our calculations, we take account the extra operators arising from the OPE at nonzero temperature and use the thermal quark, gluon, and mixed condensates up to dimension eight, as well as the temperature-dependent energy-momentum tensor.

This study is structured as follows: In Sec. II, we derive the TQCDSR for masses and residues of the spin-1/2 heavy baryons at nonzero temperature. In Sec. III, we present the numerical analysis of the obtained sum rules for the physical parameters and a comparison of our results at zero temperature with those existing in the literature. The last section is devoted to both the summary of the results and our concluding remarks.

TABLE I. Quark content of the spin-1/2 heavy baryons with different charges.

Baryon	q_1	q_2	SU(3)
$\Lambda_{b(c)}^{0(+)}$	u	d	$\bar{3}$
$\Xi_{b(c)}^{0(+)}$	u	s	$\bar{3}$
$\Xi_{b(c)}^{-(0)}$	d	s	$\bar{3}$
$\Sigma_{b(c)}^{+(++)}$	u	u	6
$\Sigma_{b(c)}^{0(+)}$	u	d	6
$\Sigma_{b(c)}^{-(0)}$	d	d	6
$\Xi_{b(c)}^{0(+)'}$	u	s	6
$\Xi_{b(c)}^{-(0)'}$	d	s	6
$\Omega_{b(c)}^{-(0)}$	s	s	6

II. THERMAL QCD SUM RULE CALCULATIONS

The aim of this section is to obtain the TQCDSR for the masses and residues of the spin-1/2 heavy Λ_Q, Ξ_Q, Σ_Q, Ξ'_Q, and Ω_Q baryons at nonzero temperature. For this purpose, we start our calculations by considering the following two-point thermal correlation function:

$$\Pi(q,T) = i \int d^4x\, e^{iq\cdot x} \langle \Psi | \mathcal{T}\{J_{B_Q}(x)\bar{J}_{B_Q}(0)\}|\Psi\rangle, \quad (1)$$

where q denotes the four-momentum of the considered spin-1/2 heavy baryon (B_Q), Ψ indicates the ground state of the hot medium, and $\mathcal{T}$ is the time-ordering operator. $J_{B_Q}(x)$ is the interpolating current of the B_Q baryon, which couples to both the positive and negative parities. It is represented by the following expressions for antitriplet ($\bar{\mathbf{3}}$) and sextet (6) baryons [29]:

$$J_{\bar{\mathbf{3}}} = \frac{1}{\sqrt{6}}\epsilon_{abc}\sum_{l=1}^{2}\{2(q_1^{T,a}(x)C\Gamma_1^l q_2^b(x))\Gamma_2^l Q^c(x) + (q_1^{T,a}(x)C\Gamma_1^l Q^b(x))\Gamma_2^l q_2^c(x) + (Q^{T,a}(x)C\Gamma_1^l q_2^b(x))\Gamma_2^l q_1^c(x)\}, \quad (2)$$

$$J_{\mathbf{6}} = -\frac{1}{\sqrt{2}}\epsilon_{abc}\sum_{l=1}^{2}\{(q_1^{T,a}(x)C\Gamma_1^l Q^b(x))\Gamma_2^l q_2^c(x) - (Q^{T,a}(x)C\Gamma_1^l q_2^b(x))\Gamma_2^l q_1^c(x)\}, \quad (3)$$

where ϵ_{abc} is the Levi-Civita tensor with color indices a, b, c, C is the charge conjugation operator, $\Gamma_1^l = 1$, $\Gamma_1^2 = \Gamma_2^1 = \gamma^5$, and $\Gamma_2^2 = t$ in which t denotes an arbitrary mixing parameter with $t = -1$ corresponding to the famous Ioffe currents that we consider in the present study. As we previously noted, q_1 and q_2 stand for light quarks and Q for the heavy quark field and they are given in Table I for all considered B_Q baryons. Thus, considering Eqs. (2) and (3), the interpolating currents for each state can be written as

$$
\begin{aligned}
J_{\Xi_Q^{-(0)}} &= -\frac{1}{\sqrt{6}}\epsilon_{abc}\sum_{l=1}^{2}\{2(d^{T,a}(x)C\Gamma_1^l s^b(x))\Gamma_2^l Q^c(x) \\
&\quad + (d^{T,a}(x)C\Gamma_1^l Q^b(x))\Gamma_2^l s^c(x) \\
&\quad + (Q^{T,a}(x)C\Gamma_1^l s^b(x))\Gamma_2^l d^c(x)\}, \\
J_{\Xi_Q^{0(+)}} &= J_{\Xi_Q^{-(0)}}(d\to u), \\
J_{\Lambda_Q^{0(+)}} &= J_{\Xi_Q^{-(0)}}(d\to u, s\to d), \\
J_{\Sigma_Q^{0(+)}} &= -\frac{1}{\sqrt{2}}\epsilon_{abc}\sum_{l=1}^{2}\{(u^{T,a}(x)C\Gamma_1^l Q^b(x))\Gamma_2^l d^c(x) \\
&\quad - (Q^{T,a}(x)C\Gamma_1^l d^b(x))\Gamma_2^l u^c(x)\}, \\
J_{\Xi_Q^{-(0)\prime}} &= J_{\Sigma_Q^{0(+)}}(u\to d, d\to s), \\
J_{\Xi_Q^{0(+)\prime}} &= J_{\Xi_Q^{-(0)\prime}}(d\to u), \\
J_{\Sigma_Q^{-(0)}} &= J_{\Xi_Q^{-(0)\prime}}(s\to d), \\
J_{\Sigma_Q^{+(++)}} &= J_{\Sigma_Q^{-(0)}}(d\to u), \\
J_{\Omega_Q^{-(0)}} &= J_{\Sigma_Q^{+(++)}}(u\to s).
\end{aligned} \tag{4}
$$

According to the standard philosophy of the QCD sum rule method, the aforementioned thermal correlation function is evaluated in two basic ways: (i) on the hadronic side, it is calculated in terms of hadronic parameters such as the temperature-dependent mass and residue of the hadron, and (ii) on the QCD side, it is calculated in terms of temperature-dependent QCD degrees of freedom in the deep Euclidean region with the help of OPE. Then, matching the coefficients of the selected structures from both sides in momentum space, via the dispersion relation, the QCD sum rules for the spectroscopic parameters of the B_Q at nonzero temperature are obtained. In the final step, to suppress the contributions of the higher states and continuum in obtained sum rules, Borel transformation and continuum subtraction are applied to both sides of these equalities. One may first apply the Borel transformation and continuum subtraction, then match the coefficients of the selected structures from both sides.

The thermal correlation function in the hadronic side is obtained by inserting the full set of hadronic states that have the same quantum numbers as the related interpolating current into Eq. (1). After performing the integration over four-x, the thermal correlation function for the hadronic side can be written as

$$
\begin{aligned}
\Pi^{\rm Had}(q,T) &= -\frac{\langle\Psi|J_{B_Q}(0)|B_Q^+(q,s)\rangle\langle B_Q^+(q,s)|J_{B_Q}^\dagger(0)|\Psi\rangle}{q^2-m_{B_Q^+}^2(T)} \\
&\quad -\frac{\langle\Psi|J_{B_Q}(0)|B_Q^-(q,s)\rangle\langle B_Q^-(q,s)|J_{B_Q}^\dagger(0)|\Psi\rangle}{q^2-m_{B_Q^-}^2(T)} \\
&\quad +\ldots,
\end{aligned} \tag{5}
$$

where $|B_Q^+(q,s)\rangle$ and $|B_Q^-(q,s)\rangle$ are spin-1/2 single heavy baryon states with positive and negative parity, respectively, the dots stand for the contributions of the higher states and continuum, and $m_{B_Q^\pm}(T)$ is the temperature-dependent mass of $B_Q^\pm$. The matrix elements $\langle\Psi|J_{B_Q}(0)|B_Q^\pm(q,s)\rangle$ for $B_Q^\pm$ are defined as

$$
\begin{aligned}
\langle\Psi|J_{B_Q}(0)|B_Q^+(q,s)\rangle &= \lambda_{B_Q^+}(T)u_{B_Q^+}(q,s), \\
\langle\Psi|J_{B_Q}(0)|B_Q^-(q,s)\rangle &= \lambda_{B_Q^-}(T)\gamma_5 u_{B_Q^-}(q,s),
\end{aligned} \tag{6}
$$

where $\lambda_{B_Q^\pm}(T)$ is the temperature-dependent residue of $B_Q^\pm$ and $u_{B_Q^\pm}(q,s)$ is the Dirac spinor of spin s and the four-momentum q. To proceed, we insert Eq. (6) into Eq. (5) and perform summation over spins of $B_Q^\pm$. The hadronic side of the thermal correlation function in its final form is decomposed in terms of different structures as

$$
\begin{aligned}
\Pi^{\rm Had}(q,T) &= -\frac{\lambda_{B_Q^+}^2(T)(\not{q}+m_{B_Q^+}(T))}{q^2-m_{B_Q^+}^2(T)} \\
&\quad -\frac{\lambda_{B_Q^-}^2(T)(-\not{q}+m_{B_Q^-}(T))}{q^2-m_{B_Q^-}^2(T)}+\cdots.
\end{aligned} \tag{7}
$$

This correlation function can be written in terms of the structures $\not{q}$ and I as

$$
\Pi^{\rm Had}(q,T) = \Pi_1^{\rm Had}(T)\not{q} + \Pi_2^{\rm Had}(T)I + \cdots, \tag{8}
$$

where $\Pi_{1(2)}^{\rm Had}(T)$, as the coefficients of the selected Lorentz structures, in the Borel scheme are obtained as

$$
\hat{B}\Pi_1^{\rm Had}(T) = \lambda_{B_Q^+}^2(T)e^{-m_{B_Q^+}^2(T)/M^2} - \lambda_{B_Q^-}^2(T)e^{-m_{B_Q^-}^2(T)/M^2}, \tag{9}
$$

and

$$
\begin{aligned}
\hat{B}\Pi_2^{\rm Had}(T) &= \lambda_{B_Q^+}^2(T)m_{B_Q^+}(T)e^{-m_{B_Q^+}^2(T)/M^2} \\
&\quad + \lambda_{B_Q^-}^2(T)m_{B_Q^-}(T)e^{-m_{B_Q^-}^2(T)/M^2},
\end{aligned} \tag{10}
$$

where M^2 is the Borel parameter to be determined in next section.

Now, we have to evaluate the QCD side of the thermal correlation function in terms of the quark-gluon degrees of freedom in the deep Euclidean region. For this aim, we insert the related interpolating current of B_Q given in Eq. (4) into Eq. (1) and contract all light and heavy quark fields using the Wick theorem. Thus, the most general form of the thermal correlation function on the QCD side, in terms of thermal light (heavy) quark propagators $S_{q(Q)}^{ij}(x)$ for $\bar{\mathbf{3}}$ and 6 baryons, are obtained as

$$\Pi_{\bar{3}}^{\mathrm{QCD}}(q,T)=\frac{i}{6}\epsilon_{abc}\epsilon_{a'b'c'}\int d^4x e^{iq\cdot x}\sum_{l=1}^{2}\sum_{k=1}^{2}\{\Gamma_2^l(2S_Q^{ca'}(x)A_1^k\tilde{S}_{q_1}^{ab'}(x)\Gamma_1^l S_{q_2}^{bc'}(x)\Gamma_2^k+2S_Q^{cb'}(x)\Gamma_1^k\tilde{S}_{q_2}^{ba'}(x)\Gamma_1^l S_{q_1}^{ac'}(x)\Gamma_2^k$$
$$-S_{q_2}^{ca'}(x)\Gamma_2^k\tilde{S}_Q^{bb'}(x)\Gamma_1^l S_{q_1}^{ac'}(x)\Gamma_1^k-2S_{q_2}^{ca'}(x)\Gamma_2^k\tilde{S}_{q_1}^{ab'}(x)\Gamma_1^l S_Q^{bc'}(x)\Gamma_1^k-S_{q_1}^{cb'}(x)\Gamma_2^k\tilde{S}_Q^{aa'}(x)\Gamma_1^l S_{q_2}^{bc'}(x)\Gamma_1^k$$
$$-2S_{q_1}^{cb'}(x)\Gamma_2^k\tilde{S}_{q_2}^{ba'}(x)\Gamma_1^l S_Q^{ac'}(x)\Gamma_1^k)-\Gamma_2^k(S_{q_1}^{cc'}(x)\Gamma_2^l\mathrm{Tr}[\Gamma_1^k S_Q^{ab'}(x)\Gamma_1^l\tilde{S}_{q_2}^{ba'}(x)]+S_{q_2}^{cc'}(x)\Gamma_2^l\mathrm{Tr}[\Gamma_1^k S_{q_1}^{ab'}(x)\Gamma_1^l\tilde{S}_Q^{ba'}(x)]$$
$$+4S_Q^{cc'}(x)\Gamma_2^l\mathrm{Tr}[\Gamma_1^k S_{q_1}^{ab'}(x)\Gamma_1^l\tilde{S}_{q_2}^{ba'}(x)])\},\tag{11}$$

$$\Pi_{\mathbf{6}}^{\mathrm{QCD}}(q,T)=-\frac{i}{2}\epsilon_{abc}\epsilon_{a'b'c'}\int d^4x e^{iq\cdot x}\sum_{l=1}^{2}\sum_{k=1}^{2}\{\Gamma_2^l(S_{q_1}^{ca'}(x)A_1^k\tilde{S}_Q^{ab'}(x)\Gamma_1^l S_{q_2}^{bc'}(x)+S_{q_2}^{cb'}(x)\Gamma_1^k\tilde{S}_Q^{ba'}(x)\Gamma_1^l S_{q_1}^{ac'}(x))\Gamma_2^k$$
$$+\Gamma_2^k(S_{q_1}^{cc'}(x)\Gamma_2^l\mathrm{Tr}[\Gamma_1^l\tilde{S}_Q^{aa'}(x)\Gamma_1^k S_{q_2}^{bb'}(x)]+S_{q_2}^{cc'}(x)\Gamma_2^l\mathrm{Tr}[\Gamma_1^l\tilde{S}_{q_1}^{aa'}(x)\Gamma_1^k S_Q^{bb'}(x)])\},\tag{12}$$

where $\tilde{S}_{q(Q)}^{ij}=CS_{q(Q)}^{ijT}C$. To proceed, thermal light (heavy) quark propagators $S_{q(Q)}^{ij}(x)$ in coordinate space are needed, which are used as (see also [48–50])

$$S_q^{ij}(x)=i\frac{\not{x}}{2\pi^2x^4}\delta_{ij}-\frac{m_q}{4\pi^2x^2}\delta_{ij}-\frac{\langle\bar{q}q\rangle_T}{12}\delta_{ij}-\frac{x^2}{192}m_0^2\langle\bar{q}q\rangle_T\left[1-i\frac{m_q}{6}\not{x}\right]\delta_{ij}+\frac{i}{3}\left[\not{x}\left(\frac{m_q}{16}\langle\bar{q}q\rangle_T-\frac{1}{12}\langle u^\mu\Theta_{\mu\nu}^f u^\nu\rangle\right)\right.$$
$$\left.+\frac{1}{3}(u\cdot x\not{u}\langle u^\mu\Theta_{\mu\nu}^f u^\nu\rangle)\right]\delta_{ij}-\frac{ig_s\lambda_A^{ij}}{32\pi^2x^2}G_{\mu\nu}^A(\not{x}\sigma^{\mu\nu}+\sigma^{\mu\nu}\not{x})-i\frac{x^2\not{x}g_s^2\langle\bar{q}q\rangle_T^2}{7776}\delta_{ij}-\frac{x^4\langle\bar{q}q\rangle_T\langle g_s^2G^2\rangle_T}{27648}+\cdots,\tag{13}$$

$$S_Q^{ij}(x)=i\int\frac{d^4k e^{-ik\cdot x}}{(2\pi)^4}\left(\frac{\not{k}+m_Q}{k^2-m_Q^2}\delta_{ij}-\frac{g_sG_{ij}^{\alpha\beta}}{4}\frac{\sigma^{\alpha\beta}(\not{k}+m_Q)+(\not{k}+m_Q)\sigma^{\alpha\beta}}{(k^2-m_Q^2)^2}+\frac{m_Q}{12}\frac{k^2+m_Q\not{k}}{(k^2-m_Q^2)^4}\langle g_s^2G^2\rangle_T\delta_{ij}+\cdots\right).\tag{14}$$

Here, $m_{q(Q)}$ is the light (heavy) quark mass, $\langle\bar{q}q\rangle_T$ is the thermal quark condensate, $\langle g_s^2G^2\rangle_T$ is thermal gluon condensate, and $m_0^2\langle\bar{q}q\rangle_T=\langle\bar{q}g_s\sigma Gq\rangle_T$ is the thermal mixed condensate. The new operators, emerging in OPE, appear to restore the Lorentz invariance broken out by the choice of the thermal rest frame at nonzero temperature. They are expressed in terms of fermionic and gluonic parts of the energy-momentum tensor $\Theta_{\mu\nu}^{f,g}$ ($\langle u^\mu\Theta_{\mu\nu}^{f,g}u^\nu\rangle=\langle u\Theta^{f,g}u\rangle=\langle\Theta_{00}^{f,g}\rangle=\langle\Theta^{f,g}\rangle$) and the four-vector velocity of the medium, u^μ. To this end, $u^\mu=(1,0,0,0)$ is chosen which leads to $u^2=1$. In the rest frame of the heat bath, $q\cdot u=q_0$, with q_0 being the energy of quasiparticle, $q_0=E_{\vec{q}}=(|\vec{q}|^2+m^2)^{1/2}$, in the mass-shell condition. At the $\vec{q}=0$ limit it is the mass of the particle. In the light quark propagator the fermionic part of the energy-momentum tensor, $\langle u^\mu\Theta_{\mu\nu}^f u^\nu\rangle$, is seen explicitly, whereas the gluonic part, $\langle u^\lambda\Theta_{\lambda\sigma}^g u^\sigma\rangle$, appears in the trace of the two-gluon field strength tensor in the heat bath [51], i.e.,

$$\langle\mathrm{Tr}^c G_{\alpha\beta}G_{\mu\nu}\rangle=\frac{1}{24}(g_{\alpha\mu}g_{\beta\nu}-g_{\alpha\nu}g_{\beta\mu})\langle G^2\rangle_T$$
$$+\frac{1}{6}[g_{\alpha\mu}g_{\beta\nu}-g_{\alpha\nu}g_{\beta\mu}-2(u_\alpha u_\mu g_{\beta\nu}-u_\alpha u_\nu g_{\beta\mu}$$
$$-u_\beta u_\mu g_{\alpha\nu}+u_\beta u_\nu g_{\alpha\mu})]\langle u^\lambda\Theta_{\lambda\sigma}^g u^\sigma\rangle.\tag{15}$$

The QCD side of the correlation function can be written similar to the hadronic side in terms of different Lorentz structures as

$$\Pi^{\mathrm{QCD}}(q,T)=\Pi_1^{\mathrm{QCD}}(T)\not{q}+\Pi_2^{\mathrm{QCD}}(T)I,\tag{16}$$

where $\Pi_{1(2)}^{\mathrm{QCD}}(T)$ are the coefficients of the selected Lorentz structures and they contain both the perturbative and nonperturbative contributions. The perturbative, and some nonperturbative, parts are written in terms of the dispersion integrals in the present study. Thus,

$$\Pi_{1(2)}^{\mathrm{QCD}}(T)=\int_{s_{\min}}^{\infty}ds\frac{\rho_{1(2)}^{\mathrm{QCD}}(s,T)}{s-q^2}+\Gamma_{1(2)}^{\mathrm{QCD}}(T),\tag{17}$$

where $s_{\min}=(m_{q_1}+m_{q_2}+m_Q)^2$, $\rho_{1(2)}^{\mathrm{QCD}}(s,T)$ are the spectral densities, and $\Gamma_{1(2)}^{\mathrm{QCD}}(T)$ stand for the remaining nonperturbative contributions that are calculated directly by applying the Borel transformation. The related spectral densities are defined as

$$\rho_{1(2)}^{\mathrm{QCD}}(s,T)=\frac{1}{\pi}\mathrm{Im}[\Pi_{1(2)}^{\mathrm{QCD}}(T)].\tag{18}$$

After the Borel transformation and continuum subtraction we get

$$\hat{B}\Pi_{1(2)}^{\mathrm{QCD}}(T)=\int_{s_{\min}}^{s_0(T)}ds\rho_{1(2)}^{\mathrm{QCD}}(s,T)e^{-s/M^2}+\hat{B}\Gamma_{1(2)}^{\mathrm{QCD}}(T),\tag{19}$$

where $s_0(T)$ is the temperature-dependent continuum threshold. The main task in this part is to find the expressions for $\rho_{1(2)}^{\mathrm{QCD}}(s,T)$ and $\hat{B}\Gamma_{1(2)}^{\mathrm{QCD}}(T)$. They are

obtained after inserting the explicit forms of the heavy and light quark propagators into the QCD side of the thermal correlation function given in Eqs. (11) and (12) for $\bar{\mathbf{3}}$ and 6 baryons with spin-1/2, performing the Fourier integral to go to the momentum space and applying the steps above to get the perturbative and nonperturbative parts. As a result, the explicit forms of the functions $\rho_{1(2)}^{\rm QCD}(s,T)$ and $\hat{B}\Gamma_{1(2)}^{\rm QCD}(T)$ are obtained. Because the obtained expressions are quite lengthy, we present the expressions of $\rho_1^{\rm QCD}(s,T)$ and $\hat{B}\Gamma_1^{\rm QCD}(T)$ for only the Σ_b^0 baryon as per an example in the Appendix.

Finally, we match the coefficients of the selected structures from the hadronic and QCD sides of the correlation function and find the sum rules:

$$\hat{B}\Pi_1^{\rm QCD}(T)=\lambda_{B_Q^+}^2(T)e^{-m_{B_Q^+}^2(T)/M^2}-\lambda_{B_Q^-}^2(T)e^{-m_{B_Q^-}^2(T)/M^2} \tag{20}$$

and

$$\hat{B}\Pi_2^{\rm QCD}(T)=\lambda_{B_Q^+}^2(T)m_{B_Q^+}(T)e^{-m_{B_Q^+}^2(T)/M^2}+\lambda_{B_Q^-}^2(T)m_{B_Q^-}(T)e^{-m_{B_Q^-}^2(T)/M^2}. \tag{21}$$

In order to obtain the four unknowns, $m_{B_Q^+}$, $m_{B_Q^-}$, $\lambda_{B_Q^+}$, and $\lambda_{B_Q^-}$, two more equations which can be achieved by applying derivatives with respect to $\frac{d}{d(-\frac{1}{M^2})}$ to both sides of Eqs. (20) and (21) are needed. Therefore, we get

$$\frac{d\Pi_1^{\rm QCD}(T)}{d(-1/M^2)}=\lambda_{B_Q^+}^2(T)m_{B_Q^+}^2(T)e^{-m_{B_Q^+}^2(T)/M^2}-\lambda_{B_Q^-}^2(T)m_{B_Q^-}^2(T)e^{-m_{B_Q^-}^2(T)/M^2}, \tag{22}$$

$$\frac{d\Pi_2^{\rm QCD}(T)}{d(-1/M^2)}=\lambda_{B_Q^+}^2(T)m_{B_Q^+}^3(T)e^{-m_{B_Q^+}^2(T)/M^2}+\lambda_{B_Q^-}^2(T)m_{B_Q^-}^3(T)e^{-m_{B_Q^-}^2(T)/M^2}, \tag{23}$$

By simultaneously solving the above four equations, the temperature-dependent masses and residues for the positive and negative parity spin-1/2 heavy baryons are obtained in terms of $s_0(T)$, M^2, QCD degrees of freedom, and other inputs. For the masses, as examples, we get

$$m_{B_Q^+}=\frac{(\alpha_4\alpha_1-\alpha_3\alpha_2+\sqrt{4\alpha_3^3\alpha_1+\alpha_4^2\alpha_1^2-6\alpha_3\alpha_4\alpha_1\alpha_2-3\alpha_3^2\alpha_2^2+4\alpha_4\alpha_2^3})}{2\alpha_3\alpha_1-2\alpha_2^2}, \tag{24}$$

$$m_{B_Q^-}=\frac{(-\alpha_4\alpha_1+\alpha_3\alpha_2+\sqrt{4\alpha_3^3\alpha_1+\alpha_4^2\alpha_1^2-6\alpha_3\alpha_4\alpha_1\alpha_2-3\alpha_3^2\alpha_2^2+4\alpha_4\alpha_2^3})}{2\alpha_3\alpha_1-2\alpha_2^2}, \tag{25}$$

where

$$\alpha_1=\hat{B}\Pi_1^{\rm QCD}(T),\qquad \alpha_2=\hat{B}\Pi_2^{\rm QCD}(T),$$
$$\alpha_3=\frac{d\Pi_1^{\rm QCD}(T)}{d(-1/M^2)},\qquad \alpha_4=\frac{d\Pi_2^{\rm QCD}(T)}{d(-1/M^2)}. \tag{26}$$

Similar results are obtained for the temperature-dependent residues.

III. NUMERICAL RESULTS

In this section, we perform the numerical analyses of the sum rules for the masses and residues of the spin-1/2 heavy Λ_Q, Ξ_Q, Σ_Q, Ξ_Q', and Ω_Q baryons at nonzero temperature. For this aim, we first use the numerical values of some input parameters collected in Table II in our calculations.

To go further in the analyses, we also need to know the thermal quark condensates $\langle\bar{q}q\rangle_T$ (for $q=u$, d, and s), parametrized in terms of vacuum condensates and temperature. For this purpose, we use the following parametrization, which is based on lattice QCD results presented in Ref. [52]:

$$\langle\bar{q}q\rangle_T=(Ae^{\frac{T}{B[\rm GeV]}}+C)\langle 0|\bar{q}q|0\rangle, \tag{27}$$

where the coefficients A, B, and C for the corresponding $q=u$, d, and s are given in Table III. Note, that the lattice results in Ref. [52] are given in a wide range of the temperatures, however, we find their fit functions up to the critical temperature under consideration in the present study (see also [47]). The above fit, together with the

TABLE II. Numerical values for the energy of quasiparticles in medium, quark masses, and vacuum condensates [1,52–55]. In the rest of the frames of the heat bath and the particle, we set the energy of the quasiparticle to its ground state positive parity mass value at each channel.

Parameters	Values
$q_0^{\Lambda_b}$; $q_0^{\Lambda_c}$	(5619.6 ± 0.17); (2286.46 ± 0.14) MeV
$q_0^{\Xi_b}$; $q_0^{\Xi_c}$	(5791.9 ± 0.5); (2467.71 ± 0.23) MeV
$q_0^{\Sigma_b}$; $q_0^{\Sigma_c}$	(5810.56 ± 0.25); (2452.9 ± 0.4) MeV
$q_0^{\Xi_b'}$; $q_0^{\Xi_c'}$	$(5935.02 \pm 0.02 \pm 0.05)$; (2578.7 ± 0.5) MeV
$q_0^{\Omega_b}$; $q_0^{\Omega_c}$	(6046.1 ± 1.7); (2695.2 ± 1.7) MeV
m_u; m_d	$(2.3^{+0.7}_{-0.5})$ MeV; $(4.8^{+0.7}_{-0.3})$ MeV
m_s	(93^{+11}_{-5}) MeV
m_b; m_c	$(4.18^{+0.04}_{-0.03})$ GeV; $(1.275^{+0.025}_{-0.035})$ GeV
m_0^2;	(0.8 ± 0.2) GeV^2
$\langle 0\|\bar{q}q\|0\rangle (q = u, d)$	$-(0.24 \pm 0.01)^3$ GeV^3
$\langle 0\|\bar{s}s\|0\rangle$	$-0.8(0.24 \pm 0.01)^3$ GeV^3
$\langle 0\|\frac{1}{\pi}\alpha_s G^2\|0\rangle$	$0.012(3)$ GeV^4

TABLE III. The coefficients A, B, and C in the thermal quark condensates $\langle \bar{q}q \rangle_T$.

	A	B [GeV]	C
For $q = u, d$	-6.534×10^{-4}	0.025	1.015
For $q = s$	-2.169×10^{-5}	0.019	1.002

parameters in Table III, exactly reproduce the graphics for the temperature-dependent quark condensates in Ref. [52].

The temperature-dependent gluon condensate $\langle G^2 \rangle_T$ is given as [52]

$$\delta\left\langle \frac{\alpha_s}{\pi} G^2 \right\rangle_T = -\frac{8}{9}[\delta T_\mu^\mu(T) - m_u \delta\langle \bar{u}u \rangle_T - m_d \delta\langle \bar{d}d \rangle_T - m_s \delta\langle \bar{s}s \rangle_T], \quad (28)$$

where

$$\delta f(T) \equiv f(T) - f(0), \quad (29)$$

and $\delta T_\mu^\mu(T)$ is defined as

$$\delta T_\mu^\mu(T) = \varepsilon(T) - 3p(T), \quad (30)$$

with $\varepsilon(T)$ being the energy density and where $p(T)$ is the pressure. Using the recent Lattice calculations given in [56,57], we obtain the following fit function for $\delta T_\mu^\mu(T)$ (see also [47]):

TABLE IV. The coefficients D, E, and F in Eq. (33).

	D	E [Gev]	F
For $\langle \Theta^f \rangle$	0.009	0.040	0.024
For $\langle \Theta^g \rangle$	0.091	0.047	−0.731

$$\delta T_\mu^\mu(T) = (0.020 e^{\frac{T}{0.034[\mathrm{GeV}]}} + 0.115) T^4. \quad (31)$$

Note that this function, obtained in the present study, exactly reproduces the lattice QCD graphics for $\delta T_\mu^\mu(T)$ with respect to temperature presented in Refs. [56,57]. The temperature-dependent strong coupling is also given as [58,59]

$$g_s^{-2}(T) = \frac{11}{8\pi^2} \ln\left(\frac{2\pi T}{\Lambda_{\overline{MS}}}\right) + \frac{51}{88\pi^2} \ln\left[2 \ln\left(\frac{2\pi T}{\Lambda_{\overline{MS}}}\right)\right], \quad (32)$$

where, $\Lambda_{\overline{MS}} \simeq T_{pc}/1.14$.

We use the results on the thermal behavior of the energy-momentum tensor given by lattice QCD in Ref. [56] and parametrize the gluonic and fermionic parts of the energy density up to the pseudocritical temperature. Hence, we use

$$\langle \Theta^{f(g)} \rangle = (D e^{\frac{T}{E[\mathrm{GeV}]}} + F) T^4, \quad (33)$$

with the related coefficients defined in Table IV. This function, obtained in the present study, reproduces the temperature-dependent energy densities presented in Ref. [56] by graphics.

In the next step, we have to obtain the temperature-dependent continuum threshold $s_0(T)$. For this purpose, we use the following parametrization:

$$s_0(T) = s_0 f(T), \quad (34)$$

where s_0 is the continuum threshold at zero temperature. It is not totally arbitrary and depends on the energy of the first excited state that lies just above the considered positive and negative parity states with the same quantum numbers. $s_0(T)$ should reduce to s_0 at the $T \to 0$ limit and $f(T)$ must obey $f(T) \to 1$ at this limit. As we mentioned in the previous section, the four unknowns (masses of the positive and negative parity baryons, as well as their residues) at each channel are obtained in terms of the Borel parameter, QCD degrees of freedom, and $s_0(T)$. As it is seen, the temperature-dependent continuum threshold, $s_0(T)$, contains the vacuum continuum threshold and $f(T)$. The s_0 together with M^2 are determined considering the standard prescriptions of the method and will be discussed below. One of the main tasks is to determine the function $f(T)$, which plays an important role in determination of the behavior of the physical quantities with respect to the temperature. To determine $f(T)$ we apply another derivative with respect to $\frac{d}{d(-\frac{1}{M^2})}$ to both sides of Eq. (22) and use

the expressions of the masses and residues, obtained in the previous section that also contain $f(T)$ though $s_0(T)$, in the resultant equation. By the numerical solving of the obtained equation at a different temperature (up to the pseudocritical temperature used in the present study), we find the following fit function for $f(T)$:

$$f(T) = 1 - 0.96\left(\frac{T}{T_{pc}}\right)^9. \tag{35}$$

Let us now discuss how we determine the working windows for the Borel parameter and the vacuum continuum threshold s_0. They are fixed using the standard criteria of the method, namely the pole dominance, OPE convergence, and weak dependence of the physical quantities on these parameters. All of these requirements lead to the following working intervals for different members of the baryons under study:

$$\begin{aligned}
43.0\ \text{GeV}^2 &\leq s_0^{\Lambda_b} \leq 44.0\ \text{GeV}^2,\\
44.0\ \text{GeV}^2 &\leq s_0^{\Sigma_b} \leq 46.0\ \text{GeV}^2,\\
45.0\ \text{GeV}^2 &\leq s_0^{\Xi_b} \leq 46.0\ \text{GeV}^2,\\
47.0\ \text{GeV}^2 &\leq s_0^{\Xi_b'} \leq 48.0\ \text{GeV}^2,\\
48.5\ \text{GeV}^2 &\leq s_0^{\Omega_b} \leq 49.5\ \text{GeV}^2,\\
M^2 &\in [5,8]\ \text{GeV}^2,
\end{aligned} \tag{36}$$

for the bottom and

$$\begin{aligned}
8.5\ \text{GeV}^2 &\leq s_0^{\Lambda_c} \leq 9.5\ \text{GeV}^2,\\
9.5\ \text{GeV}^2 &\leq s_0^{\Sigma_c} \leq 10.5\ \text{GeV}^2,\\
10.5\ \text{GeV}^2 &\leq s_0^{\Xi_c} \leq 11.5\ \text{GeV}^2,\\
11.5\ \text{GeV}^2 &\leq s_0^{\Xi_c'} \leq 12.5\ \text{GeV}^2,\\
11.8\ \text{GeV}^2 &\leq s_0^{\Omega_c} \leq 12.8\ \text{GeV}^2,\\
M^2 &\in [3,5]\ \text{GeV}^2,
\end{aligned} \tag{37}$$

for the charmed baryons. To check the stability of the results with respect to the changes in M^2 and s_0 in their working intervals, as an example, we plot a three-dimensional (3D) graphic of the mass of the Σ_b^0 positive parity baryon as functions of these auxiliary parameters at $T = 0$ in Fig. 1. We see that the dependence of the mass on both M^2 and s_0 is weak and the changes remain within the acceptable limits of the method. The parameters of other members show similar behavior.

Now, we proceed to investigate the temperature dependence of the masses and residues of the B_Q baryons. As examples, we only present the results on the temperature-dependent masses and residues for the positive parity baryons. They reflects behavior of the OPE sides, which

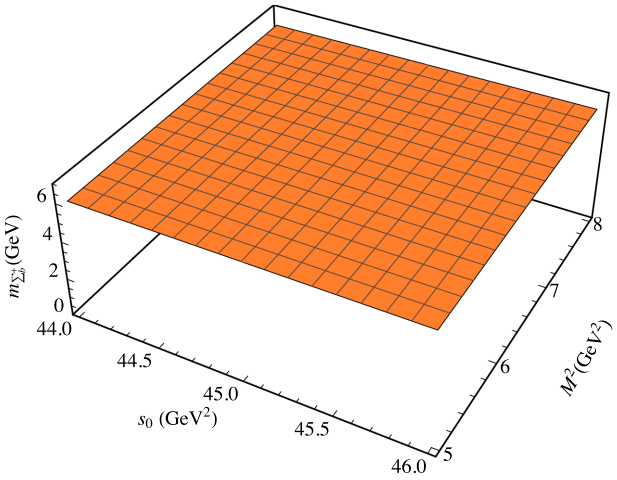

FIG. 1. The mass of the positive parity Σ_b baryon as functions of M^2 and s_0 at $T = 0$.

are common for both the positive and negative parity baryons, i.e., the masses and residues of both parities are obtained in terms of the functions in OPE sides as presented in the previous section. To this end, we plot the ratio of the temperature-dependent mass (residue) to its vacuum value, $m(T)/m(0)$ $(\lambda(T)/\lambda(0))$, for the positive parity baryons as functions of M^2 and ratio T/T_{pc} in 3D at average values of s_0 for Λ_b, Ξ_b, Σ_b, Ξ_b', and Ω_b baryons in Figs. 2 and 3. From these figures, we see that the spectroscopic parameters of these baryons remain approximately unchanged with respect to the changes in T/T_{pc} up to $T \cong 108$ MeV for masses and $T \cong 93$ MeV for residues. After these points, they start to decrease rapidly with increasing the temperature and we are witness to the melting of these baryons. We realize that a similar situation is valid for the charmed Λ_c, Ξ_c, Σ_c, Ξ_c', and Ω_c baryons. The amount of negative shifts in masses and residues near to the critical point are shown in Tables V and VI. In the case of mass, the order of shifts are roughly comparable between the bottom and charmed baryons of each channel. Among the results, the order of negative shifts for all channels in the bottom case is roughly the same but shows some differences among the charmed baryons. The sum rules for masses give reliable predictions up to the pseudocritical point considered in the present study. As far as the residues are concerned, the amount of shifts are roughly the same for b- and c-baryons and they are very large. Thus, at $T \to T_{pc}$ limit, the residues approach to zero and we see the melting of the baryons.

Our final task in this section is to discuss the results at the $T \to 0$ limit. In this limit, the values of masses for the spin-1/2 heavy baryons containing a bottom quark with both the positive and negative parities are presented in Tables VII and VIII, respectively. Similarly, the vacuum masses for the spin-1/2 heavy baryons containing a charm quark with both the positive and negative parities are presented in

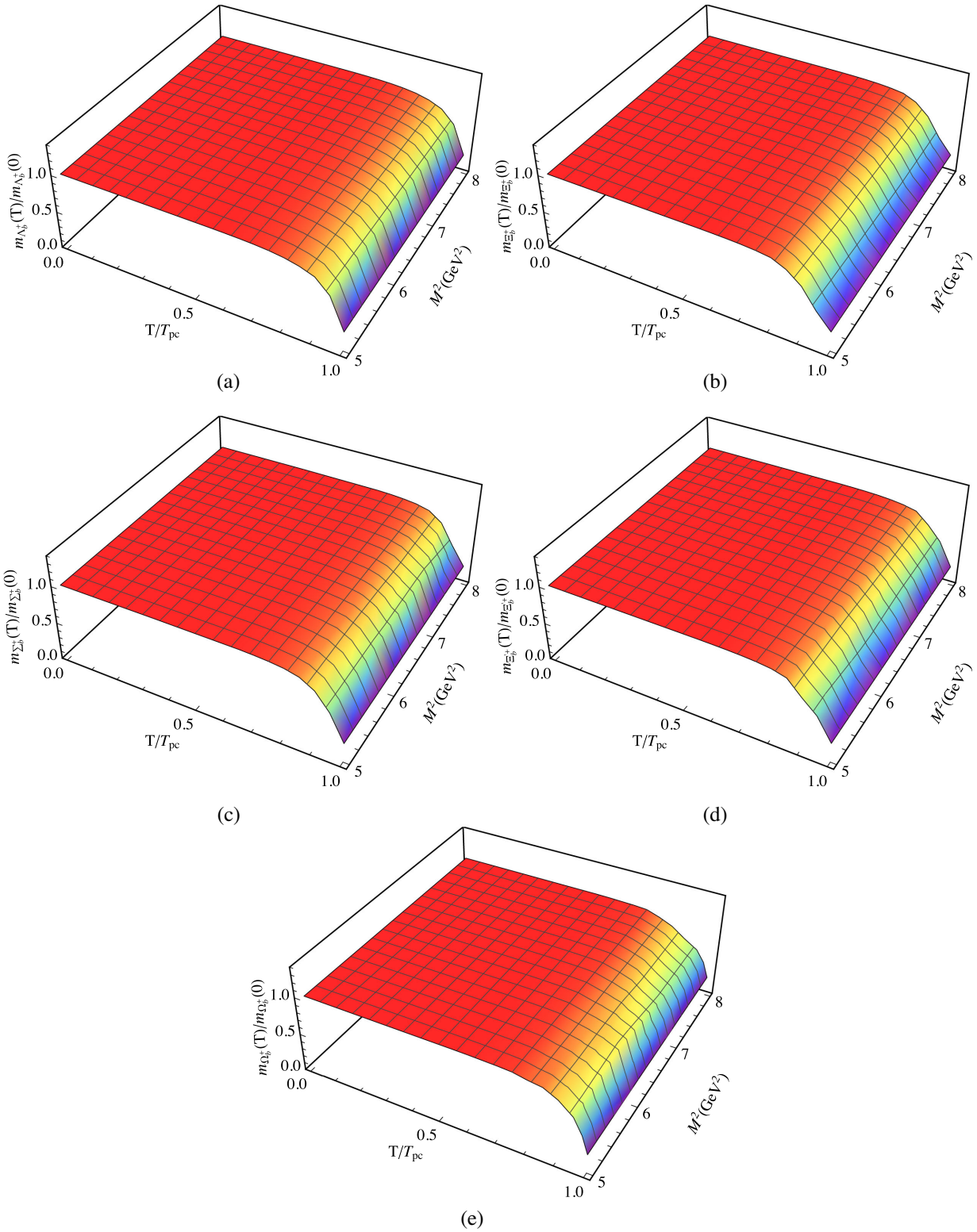

FIG. 2. The ratio $m(T)/m(0)$ as functions of M^2 and T/T_{pc} for positive parity Λ_b, Ξ_b, Σ_b, Ξ_b', and Ω_b baryons at the average value of s_0.

Tables IX and X, respectively. From these tables, we see that our results are in good consistency with existing experimental data and other theoretical predictions within the presented uncertainties. These consistencies lead us to hope that the obtained results at nonzero temperature in the present study can shed light on the future heavy ion

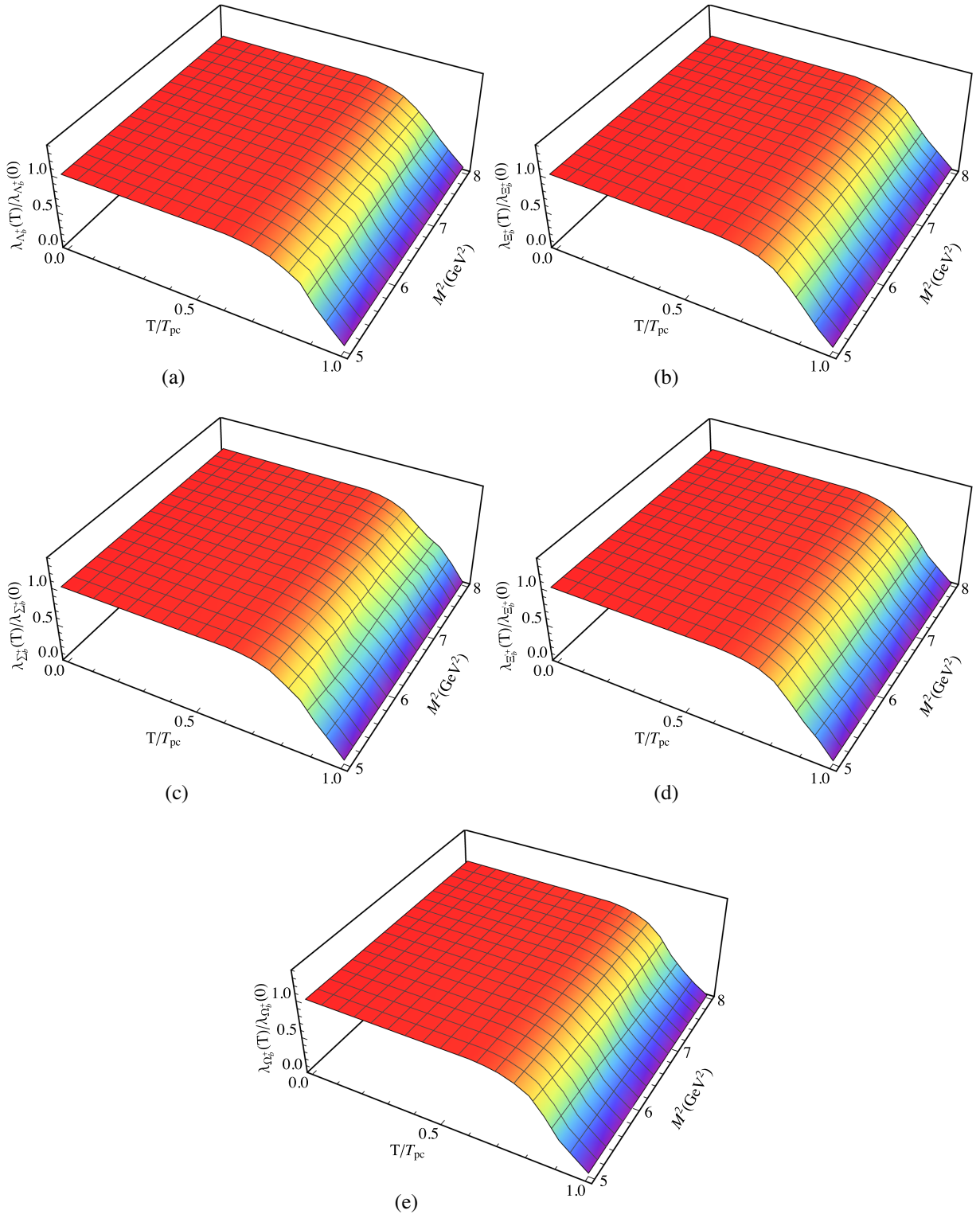

FIG. 3. The ratio $\lambda(T)/\lambda(0)$ as functions of M^2 and T/T_{pc} for positive parity Λ_b, Ξ_b, Σ_b, Ξ_b', and Ω_b baryons at the average value of s_0.

collision experiments and can be used in analyses of the related data. The uncertainties in our predictions belong to those related to the working intervals of the auxiliary parameters as well as the uncertainties of all the presented input parameters.

IV. SUMMARY AND CONCLUSIONS

We investigated the mass and residue of the spin-1/2 single heavy Λ_Q, Ξ_Q, Σ_Q, Ξ_Q', and Ω_Q baryons as functions of temperature in the framework of the thermal QCD sum

TABLE V. At the $T \to T_{pc}$ limit, the percent of negative shifts in masses of the spin-1/2 heavy baryons with the positive parity compared to their vacuum values.

	$\Lambda^+_{b(c)}$	$\Xi^+_{b(c)}$	$\Sigma^+_{b(c)}$	$\Xi'^+_{b(c)}$	$\Omega^+_{b(c)}$
Negative shift (%)	74(72)	74(72)	74(80)	74(77)	75(77)

TABLE VI. The percent of negative shifts in residues of the spin-1/2 heavy baryons with the positive parity relative to their vacuum values near the pseudocritical point.

	$\Lambda^+_{b(c)}$	$\Xi^+_{b(c)}$	$\Sigma^+_{b(c)}$	$\Xi'^+_{b(c)}$	$\Omega^+_{b(c)}$
Negative shift (%)	92	94	96	97	96

rule. In our calculations, we took into account the nonperturbative operators up to mass dimension 8, including those arising from the Wilson expansion at finite temperature due to breaking the Lorentz invariance. The obtained results indicate that the mass of these baryons in both the bottom and charm channels remain stable up to roughly $T = 108$ MeV while their residue is unchanged up to $T = 93$ MeV. After these points, the masses and residues start to diminish by increasing in temperature. The shifts in the mass and residue for both the bottom and charm channels are considerably large, and we observe the melting of these baryons near to the pseudocritical temperature determined by recent lattice QCD calculations. The amount of negative shifts near to the pseudocritical point have been shown in Tables V and VI. The order of shifts in masses are roughly the same between the bottom and charmed baryons of each channel. Among the results, the order of shifts for all channels for bottom baryons is roughly the same but shows some differences among the charmed members. The sum rules for masses give reliable predictions up to the pseudocritical point considered in the present study (roughly 155 MeV). As far as the residues are concerned, the amount of shifts in bottom and charmed cases of each channel are the same. The negative shifts near to the end point are very large for all baryons and the residues approach to zero at the pseudocritical point.

We presented our results for the mass of the single heavy baryons with both the positive and negative parities at the $T \to 0$ limit in Tables VII, VIII, IX, and X. We observed that the obtained results for the single heavy bottom and charmed baryons of spin-1/2 with both the positive and negative parities in the present study are in good

TABLE VII. Vacuum masses of the spin-1/2 positive parity heavy baryons containing a bottom quark (in GeV).

	$m_{\Lambda^+_b}$	$m_{\Xi^+_b}$	$m_{\Sigma^+_b}$	$m_{\Xi'^+_b}$	$m_{\Omega^+_b}$
Present work	$5.691^{+0.101}_{-0.109}$	$5.797^{+0.078}_{-0.077}$	$5.845^{+0.137}_{-0.144}$	$5.957^{+0.147}_{-0.157}$	$6.065^{+0.113}_{-0.112}$
Exp [1]	5.61960 ± 0.00017	5.7919 ± 0.0005	5.81056 ± 0.00025	$5.93502 \pm 0.00002 \pm 0.00005$	6.0461 ± 0.0017
[2]	5.612	5.844	5.833	⋯	6.081
[3]	⋯	5.790–5800	⋯	5.930 ± 0.005	6.0521 ± 0.0056
[4]	5.585	⋯	5.795	⋯	⋯
[5]	⋯	⋯	5.83 ± 0.09	⋯	⋯
[6]	$5.637^{+0.068}_{-0.056}$	$5.780^{+0.073}_{-0.068}$	$5.809^{+0.082}_{-0.076}$	$5.903^{+0.081}_{-0.079}$	6.036 ± 0.081
[7]	5.641 ± 0.05	5.80	5.82	5.94	6.04
[9]	5.620 ± 0.040	5.810 ± 0.040	5.820 ± 0.040	5.950 ± 0.040	6.060 ± 0.050
[10]	⋯	5.833	5.815	–	5.948
[11]	5.683	5.833	5.708	–	5.967
[14]	5.626	5.771	5.856	5.933	6.056
[15]	5.664	5.762	⋯	⋯	6.021
[18]	5.622	5.812	5.805	5.937	6.065
[19]	5.622	5.812	5.805	⋯	6.065
[20]	5.620	5.803	5.808	⋯	6.064
[26]	5.609	5.8036	5.8055	5.9338	6.0571
[27]	5.62	5.75	5.75	5.88	6.00
[30]	5.614 ± 0.345	⋯	5.810 ± 0.241	⋯	⋯
[31,32]	$5.618^{+0.078}_{-0.104}$	⋯	5.96 ± 0.10	⋯	⋯
[33]	5.65 ± 0.20	5.73 ± 0.18	⋯	⋯	⋯
[34,35]	5.69 ± 0.13	5.75 ± 0.13	5.73 ± 0.21	5.87 ± 0.20	5.89 ± 0.18
[37]	⋯	⋯	⋯	⋯	6.487 ± 0.187
[39]	⋯	⋯	⋯	⋯	6.024 ± 0.065

TABLE VIII. Vacuum masses of the spin-1/2 negative parity heavy baryons containing a bottom quark (in GeV).

	$m_{\Lambda_b^-}$	$m_{\Xi_b^-}$	$m_{\Sigma_b^-}$	$m_{\Xi_b'^-}$	$m_{\Omega_b^-}$
Present work	$5.910^{+0.118}_{-0.132}$	$6.095^{+0.135}_{-0.150}$	$6.143^{+0.095}_{-0.087}$	$6.255^{+0.113}_{-0.104}$	$6.370^{+0.066}_{-0.061}$
Exp [1]	5.91219 ± 0.00017	⋯	⋯	⋯	⋯
[2]	5.939	6.108	6.099	⋯	6.301
[4]	5.912	⋯	6.070	⋯	⋯
[19]	5.930	6.119	6.108	⋯	6.352
[20]	5.930	6.120	6.101	⋯	6.339
[25]	5.890	6.076	6.039	⋯	6.278
[27]	6.03	6.15	6.32	6.40	6.49
[33]	5.85 ± 0.18	6.01 ± 0.16	⋯	⋯	⋯
[34,35]	5.85 ± 0.15	5.95 ± 0.16	⋯	⋯	⋯
[37]	⋯	⋯	⋯	⋯	6.336 ± 0.183

consistency with the experimental data presented in Ref. [1], as well as with other theoretical predictions made via different phenomenological approaches. Our results on the behavior of the physical quantities considered in the present study, with respect to temperature and the amount of shifts in these quantities near the pseudocritical point, may be checked via other phenomenological approaches. The obtained results in the present study may shed light on analyses of the data provided by the future heavy ion collision experiments.

TABLE IX. Vacuum masses of the spin-1/2 positive parity heavy baryons containing a charm quark (in GeV).

	$m_{\Lambda_c^+}$	$m_{\Xi_c^+}$	$m_{\Sigma_c^+}$	$m_{\Xi_c'^+}$	$m_{\Omega_c^+}$
Present work	$2.283^{+0.087}_{-0.095}$	$2.460^{+0.025}_{-0.094}$	$2.488^{+0.105}_{-0.113}$	$2.576^{+0.095}_{-0.101}$	$2.689^{+0.100}_{-0.093}$
Exp [1]	2.28646 ± 0.00014	2.46771 ± 0.00023	2.4529 ± 0.0004	2.5787 ± 0.0005	2.6952 ± 0.0017
[2]	2.268	2.492	2.455	⋯	2.718
[4]	2.265	⋯	2.440	⋯	⋯
[5]	⋯	⋯	2.52 ± 0.08	2.5808 ± 0.0021	⋯
[6]	$2.271^{+0.067}_{-0.049}$	$2.432^{+0.079}_{-0.068}$	$2.411^{+0.093}_{-0.081}$	$2.508^{+0.097}_{-0.091}$	$2.657^{+0.102}_{-0.099}$
[7]	2.285 ± 0.0006	2.4728 ± 0.0017	2.4525 ± 0.0009	2.57	$2.719 \pm 0.007 \pm 0.0025$
[9]	2.285 ± 0.001	2.468 ± 0.003	2.453 ± 0.003	2.580 ± 0.020	2.710 ± 0.030
[10]	⋯	2.473	2.455	⋯	2.588
[11]	2.303	2.453	2.328	⋯	2.587
[12]	⋯	2.653	2.586	⋯	2.720
[13]	⋯	2.648	2.575	⋯	2.723
[14]	2.254	2.433	2.474	2.574	2.679
[15]	⋯	2.440	2.407	⋯	2.652
[16]	2.295	2.462	2.490	2.594	2.699
[17]	2.343(23)	2.474(11)	2.459(45)	2.593(22)	2.711(16)
[18,19]	2.297	2.481	2.439	2.578	2.698
[20]	2.286	2.476	2.443	⋯	2.698
[26]	2.2807	2.4752	2.4485	2.5768	2.7001
[27]	2.40	2.55	2.45	2.59	2.73
[30]	2.295 ± 0.251	⋯	2.451 ± 0.208	⋯	⋯
[31,32]	$2.284^{+0.049}_{-0.078}$	⋯	2.54 ± 0.15	⋯	⋯
[33]	2.26 ± 0.27	2.44 ± 0.23	⋯	⋯	⋯
[34,35]	2.31 ± 0.19	2.48 ± 0.21	2.40 ± 0.31	2.50 ± 0.29	2.62 ± 0.29
[36]	⋯	⋯	⋯	2.925 ± 0.115	⋯
[38,39]	⋯	⋯	⋯	⋯	2.685 ± 0.123

TABLE X. Vacuum masses of the spin-1/2 negative parity heavy baryons containing a charm quark (in GeV).

	$m_{\Lambda_c^-}$	$m_{\Xi_c^-}$	$m_{\Sigma_c^-}$	$m_{\Xi_c'^-}$	$m_{\Omega_c^-}$
Present work	$2.548^{+0.090}_{-0.086}$	$2.763^{+0.103}_{-0.102}$	$2.868^{+0.051}_{-0.037}$	$2.901^{+0.082}_{-0.079}$	$3.099^{+0.046}_{-0.024}$
Exp [1]	2.59225 ± 0.00028	2.7919 ± 0.0005	...	...	...
[2]	2.625	2.763	2.748	...	2.977
[4]	2.630	...	2.795	...	...
[17]	2.668(16)	2.770(67)	2.814(20)	2.933(16)	3.044(15)
[19]	2.598	2.801	2.795	...	3.020
[20]	2.598	2.792	2.799	...	3.055
[21]	2.594	2.769	2.769	...	...
[22–24]	2.400	...	2.700	...	...
[25]	2.559	2.749	2.706	...	2.959
[27]	2.67	2.79	2.84	2.94	3.03
[33]	2.61 ± 0.21	2.76 ± 0.18	...	...	...
[34,35]	2.53 ± 0.22	2.65 ± 0.27	...	...	...
[36]	...	...	...	2.925 ± 0.115	...
[38,39]	...	...	...	...	2.990 ± 0.129

APPENDIX

In this appendix, we present the explicit forms of the spectral density $\rho_1^{\rm QCD}(s,T)$ (for perturbative and some nonperturbative parts) and the function $\hat{B}\Gamma_1^{\rm QCD}(T)$ defining other nonperturbative contributions for the Σ_b^0 baryon as examples. They are obtained as

$$\rho_1^{\rm pert}(s,T) = -\frac{1}{64\pi^4}\int_0^1 \frac{dz}{(z-1)}\{6\beta[m_b^2 m_u m_d - \beta s m_u m_d] - 3z^2 m_b^4 - 8\beta z^2 s m_b^2 - 5\beta^2 z^2 s^2\} \times \Theta[L(s,z)], \tag{A1}$$

$$\rho_1^{\langle q\bar{q}\rangle}(s,T) = -\frac{1}{8\pi^2}\int_0^1 dz\beta\{m_u[\langle\bar{d}d\rangle - 3z\langle\bar{u}u\rangle] + m_d[\langle\bar{u}u\rangle - 3z\langle\bar{d}d\rangle]\} \times \Theta[L(s,z)], \tag{A2}$$

$$\rho_1^{\langle G^2\rangle+\langle\Theta^{f,g}\rangle}(s,T) = \frac{1}{\pi^2}\int_0^1 dz\left\{z^2\left[\frac{g_s^2}{96\pi^2}\langle u\Theta^g u\rangle - \frac{3}{32}\left\langle\frac{\alpha_s G^2}{\pi}\right\rangle\right] - \frac{z\beta}{3}\langle u\Theta^f u\rangle\right\} \times \Theta[L(s,z)]. \tag{A3}$$

Here, z is the Feynman parameter, Θ indicates the unit-step function, $L(s,z) = sz(1-z) - zm_b^2$, and $\beta = z-1$. The explicit form of the function $\hat{B}\Gamma_1^{\rm QCD}(T)$ for the Σ_b^0 baryon is obtained as

TABLE XI. List of some operators and their mass dimensions entering our calculations.

Dimension	Operator
1	I
3	$\langle\bar{q}_{1(2)}q_{1(2)}\rangle$
4	$\langle\Theta^{f(g)}\rangle$
4	$\langle G^2\rangle$
5	$m_0^2\langle\bar{q}_{1(2)}q_{1(2)}\rangle$
6	$\langle\bar{q}_1 q_1\rangle\langle\bar{q}_2 q_2\rangle$
6	$\langle\bar{q}_{1(2)}q_{1(2)}\rangle^2$
7	$\langle\bar{q}_{1(2)}q_{1(2)}\rangle\langle G^2\rangle$
7	$\langle\bar{q}_{1(2)}q_{1(2)}\rangle\langle\Theta^{f(g)}\rangle$
8	$\langle\Theta^{f(g)}\rangle^2$
8	$\langle G^2\rangle^2$
8	$\langle\Theta^{f(g)}\rangle\langle G^2\rangle$

$$\begin{aligned}\hat{B}\Gamma_1^{\mathrm{QCD}}(T) = {} & \frac{1}{1728\pi^2M^6}\int_0^1 dz \frac{e^{\frac{m_b^2}{M^2\beta}}}{\beta^6}\left\{\left\langle\frac{\alpha_s G^2}{\pi}\right\rangle(-9M^4m_u m_d m_b^2 z\beta^4 - 3\beta\pi^2 m_u m_d m_b\langle\bar{d}d\rangle[m_b^2\beta^3\right.\\
& + 3M^2\beta^4 + M^2\beta^2(1-4z+3z^2)] + m_u\langle\bar{u}u\rangle\pi^2[-63M^2\beta^2m_b^2(1-z^3) + 180M^4\beta^6 + 9m_b^4\beta^3 z\\
& - 27M^2m_b^2\beta(1+3z^3-3z^2)] + m_d\langle\bar{d}d\rangle\pi^2[M^2\beta^2m_b^2(-36++153z-198z^2+81z^3) + 108M^4\beta^4(1+z^2)\\
& + 8505M^2\beta m_b^2z^2 + 72M^4\beta^3(z^3-1-6z\beta) + 15m_b^4z\beta^3 + 45M^2\beta^4m_b^2z] - 12\pi^2M^2\beta^4m_b^2(m_u\langle\bar{d}d\rangle + m_d\langle\bar{u}u\rangle)\\
& + (12\pi^2M^2\beta^3 z m_b\langle\bar{d}d\rangle - 6\pi^2M^2\beta^3 z m_b\langle\bar{u}u\rangle)(\beta m_b^2 + 5M^2\beta + 2M^2)) - (12M^2\beta^5 g_s^2 m_b^2\langle u\Theta^g u\rangle + 36M^4\beta^6 g_s^2\langle u\Theta^g u\rangle\\
& + 48M^2\beta^6 q_0^2 g_s^2\langle u\Theta^g u\rangle)(m_u\langle\bar{u}u\rangle + m_d\langle\bar{d}d\rangle) + \langle u\Theta^f u\rangle\left[\left\langle\frac{\alpha_s G^2}{\pi}\right\rangle(M^2\pi^2\beta^2m_b^2(144-176z-80z^3+208z^2)\right.\\
& + 96M^2\pi^2\beta(m_b^2(1+3z^3-3z^2-z^4) - M^2\beta^5) + 32m_b^4z(\pi^2+3z-z^3+3z^2) - 128\pi^2\beta^4m_b^2q_0^2z\\
& + 144M^4\pi^2\beta^3z^2(2-\beta) + 48M^4\pi^2\beta^3(2-3\beta-6z)) + M^2\beta^3g_s^2\langle u\Theta^g u\rangle(80M^2\beta^3 - 416M^2\beta z + 16\beta^2m_b^2 + 256\beta^3q_0^2\\
& \left.\left. - 96\beta m_b^2 - 1536\beta^2q_0^2 - 96m_b^2 - 1536\beta q_0^2)\right]\right\}\Theta[L(s_0,z)]\\
& + \frac{e^{-\frac{m_b^2}{M^2}}}{864\pi^2M^8}\left\{27M^8m_0^2(m_u\langle\bar{d}d\rangle + m_d\langle\bar{u}u\rangle) + 144\pi^2M^8\langle\bar{u}u\rangle\langle\bar{d}d\rangle + 72\pi^2M^4[m_d\langle\bar{d}d\rangle(m_u\langle\bar{u}u\rangle(m_b^2+M^2)\right.\\
& + M^2\langle u\Theta^f u\rangle) - m_b^2m_u\langle\bar{u}u\rangle\langle u\Theta^f u\rangle - M^2m_0^2\langle\bar{u}u\rangle\langle\bar{d}d\rangle] + 3\pi^2M^4\left\langle\frac{\alpha_s G^2}{\pi}\right\rangle\langle\bar{u}u\rangle(m_b^2(m_u-m_d) - M^2(m_u+m_d))\\
& + 48\pi^2M^6m_b\langle u\Theta^f u\rangle(\langle\bar{u}u\rangle - \langle\bar{d}d\rangle) + 9\pi^2M^4m_u\langle\bar{u}u\rangle\langle u\Theta^f u\rangle(24M^2+64q_0^2)\\
& - \pi^2M^4m_d\langle\bar{d}d\rangle\langle u\Theta^f u\rangle(120m_b^2 - 384q_0^2) - 8\pi^2m_0^2m_b^2\langle\bar{u}u\rangle\langle\bar{d}d\rangle(m_b^2m_um_d + 9M^4)\\
& \left. + 128\pi^2M^4\langle u\Theta^f u\rangle^2(m_b^2 - 3M^2 - 8q_0^2)\right\}, \qquad \text{(A4)}\end{aligned}$$

where the dimensions of some operators included in the formulas are given in Table XI.

[1] P. A. Zyla *et al.* (Particle Data Group), Review of particle physics, Prog. Theor. Exp. Phys. **2020**, 083C01 (2020).

[2] W. Roberts and M. Pervin, Heavy baryons in a quark model, Int. J. Mod. Phys. A **23**, 2817 (2008).

[3] M. Karliner, B. Keren-Zura, H. J. Lipkin, and J. L. Rosner, The quark model and b baryons, Ann. Phys. (Amsterdam) **324**, 2 (2009).

[4] S. Capstick and N. Isgur, Baryons in a relativized quark model with chromodynamics, Phys. Rev. D **34**, 2809 (1986).

[5] Y. B. Dai, C. S. Huang, C. Liu, and C. D. Lu, 1m corrections to heavy baryon masses in the heavy quark effective theory sum rules, Phys. Lett. B **371**, 99 (1996).

[6] X. Liu, H. X. Chen, Y. R. Liu, A. Hosaka, and S. L. Zhu, Bottom baryons, Phys. Rev. D **77**, 014031 (2008).

[7] J. G. Körner, M. Krämer, and D. Pirjol, Heavy baryons, Prog. Part. Nucl. Phys. **33**, 787 (1994).

[8] M. J. Savage, Charmed baryon masses in chiral perturbation theory, Phys. Lett. B **359**, 189 (1995).

[9] R. Roncaglia, D. B. Lichtenberg, and E. Predazzi, Predicting the masses of baryons containing one or two heavy quarks, Phys. Rev. D **52**, 1722 (1995); R. Roncaglia, A. Dzierba, D. B. Lichtenberg, and E. Predazzi, Predicting the masses of heavy hadrons without an explicit Hamiltonian, Phys. Rev. D **51**, 1248 (1995).

[10] Z. Ghalenovi, A. A. Rajabi, and A. Tavakolinezhad, The heavy baryon masses and spin-isospin dependence, J. Phys. Conf. Ser. **347**, 012015 (2012).

[11] Z. Ghalenovi, A. A. Rajabi, and M. Hamzavi, The heavy baryon masses in variational approach and spin-isospin dependence, Acta Phys. Pol. B **42**, 1849 (2011).

[12] B. Patel, A. K. Rai, and P. C. Vinodkumar, Masses and magnetic moments of charmed baryons using hyper central model, arXiv:0803.0221.

[13] B. Patel, A. K. Rai, and P. C. Vinodkumar, Heavy flavor baryons in hypercentral model, Pramana **70**, 797 (2008).

[14] Z. S. Brown, W. Detmold, S. Meinel, and K. Orginos, Charmed bottom baryon spectroscopy from lattice QCD, Phys. Rev. D **90**, 094507 (2014).

[15] N. Mathur, R. Lewis, and R. M. Woloshyn, Charmed and bottom baryons from lattice nonrelativistic QCD, Phys. Rev. D **66**, 014502 (2002).

[16] R. Lewis, N. Mathur, and R. M. Woloshyn, Charmed baryons in lattice QCD, Phys. Rev. D **64**, 094509 (2001).
[17] H. Bahtiyar, K. U. Can, G. Erkol, P. Gubler, M. Oka, and T. T. Takahashi, Charmed baryon spectrum from lattice QCD near the physical point, Phys. Rev. D **102**, 054513 (2020).
[18] D. Ebert, R. N. Faustov, and V. O. Galkin, Masses of heavy baryons in the relativistic quark model, Phys. Rev. D **72**, 034026 (2005).
[19] D. Ebert, R. N. Faustov, and V. O. Galkin, Masses of excited heavy baryons in the relativistic quark-diquark picture, Phys. Lett. B **659**, 612 (2008).
[20] D. Ebert, R. N. Faustov, and V. O. Galkin, Spectroscopy and Regge trajectories of heavy baryons in the relativistic quark-diquark picture, Phys. Rev. D **84**, 014025 (2011).
[21] S. Migura, D. Merten, B. Metsch, and H. R. Petry, Charmed baryons in a relativistic quark model, Eur. Phys. J. A **28**, 41 (2006).
[22] S. M. Gerasyuta and D. V. Ivanov, Charmed baryons in bootstrap quark model, Nuovo Cimento A **112**, 261 (1999).
[23] S. M. Gerasyuta and E. E. Matskevich, Charmed $(70, 1^-)$ baryon multiplet, Int. J. Mod. Phys. E **17**, 585 (2008).
[24] S. M. Gerasyuta and E. E. Matskevich, S-wave bottom baryons, Int. J. Mod. Phys. E **18**, 1785 (2009).
[25] H. Garcilazo, J. Vijande, and A. Valcarce, Faddeev study of heavy-baryon spectroscopy, J. Phys. G **34**, 961 (2007).
[26] J. Y. Kim, H. C. Kim, and G. S. Yang, Mass spectra of singly heavy baryons in a self-consistent chiral quark-soliton model, Phys. Rev. D **98**, 054004 (2018).
[27] P.-L. Yin, Z.-F. Cui, C. D. Roberts, and J. Segovia, Masses of positive- and negative-parity hadron ground-states, including those with heavy quarks, Eur. Phys. J. C **81**, 327 (2021).
[28] E. V. Shuryak, Hadrons containing a heavy quark and QCD sum rules, Nucl. Phys. **B198**, 83 (1982).
[29] E. Bagan, M. Chabab, H. G. Dosch, and S. Narison, The Heavy baryons $\Sigma_{c,b}$ from QCD spectral sum rules, Phys. Lett. B **278**, 367 (1992).
[30] K. Azizi, N. Er, and H. Sundu, Scalar and vector self-energies of heavy baryons in nuclear medium, Nucl. Phys. **A960**, 147 (2017).
[31] Z. G. Wang, Analysis of Σ_Q baryons in nuclear matter with QCD sum rules, Phys. Rev. C **85**, 045204 (2012).
[32] Z. G. Wang, Analysis of the Λ_Q baryons in the nuclear matter with the QCD sum rules, Eur. Phys. J. C **71**, 1816 (2011).
[33] Z. G. Wang, Analysis of the $\frac{1}{2}^{\pm}$ flavor antitriplet heavy baryon states with QCD sum rules, Eur. Phys. J. C **68**, 479 (2010).
[34] J. R. Zhang and M. Q. Huang, Mass spectra of the heavy baryons Λ_Q and $\Sigma_Q^{(*)}$ from QCD sum rules, Phys. Rev. D **77**, 094002 (2008).
[35] J. R. Zhang and M. Q. Huang, Heavy baryon spectroscopy in QCD, Phys. Rev. D **78**, 094015 (2008).
[36] S. S. Agaev, K. Azizi, and H. Sundu, Newly discovered Ξ_c^0 resonances and their parameters, Eur. Phys. J. A **57**, 201 (2021).
[37] S. S. Agaev, K. Azizi, and H. Sundu, Decay widths of the excited Ω_b baryons, Phys. Rev. D **96**, 094011 (2017).
[38] S. S. Agaev, K. Azizi, and H. Sundu, Interpretation of the new Ω_c^0 states via their mass and width, Eur. Phys. J. C **77**, 395 (2017).
[39] S. S. Agaev, K. Azizi, and H. Sundu, On the nature of the newly discovered Ω_c^0 states, Europhys. Lett. **118**, 61001 (2017).
[40] Y. Aoki, G. Endrődi, Z. Fodor, S. D. Katz, and K. K. Szabó, The order of the quantum chromodynamics transition predicted by the standard model of particle physics, Nature (London) **443**, 675 (2006).
[41] M. Cheng *et al.*, Transition temperature in QCD, Phys. Rev. D **74**, 054507 (2006).
[42] T. Bhattacharya *et al.*, QCD Phase Transition with Chiral Quarks and Physical Quark Masses, Phys. Rev. Lett. **113**, 082001 (2014).
[43] A. Bazavov *et al.*, QCD equation of state to $\mathcal{O}(\mu_B^6)$ from lattice QCD, Phys. Rev. D **95**, 054504 (2017).
[44] A. I. Bochkarev and M. E. Shaposhnikov, The spectrum of hot hadronic matter and finite-temperature QCD sum rules, Nucl. Phys. **B268**, 220 (1986).
[45] M. A. Shifman, A. I. Vainstein, and V. I. Zakharov, QCD and resonance physics. theoretical foundations, Nucl. Phys. **B147**, 385 (1979); M. A. Shifman, A. I. Vainstein, and V. I. Zakharov, QCD and resonance physics. applications, Nucl. Phys. **B147**, 448 (1979).
[46] B. L. Ioffe, Calculation of baryon masses in quantum chromodynamics, Nucl. Phys. **B188**, 317 (1981).
[47] K. Azizi and A. Türkan, S-wave single heavy baryons with spin-3/2 at finite temperature, Eur. Phys. J. C **80**, 425 (2020).
[48] K. Azizi and G. Kaya, Thermal behavior of the mass and residue of hyperons, J. Phys. G **43**, 055002 (2016).
[49] K. Azizi, A. Türkan, E. Veli Veliev, and H. Sundu, Thermal properties of light tensor mesons via QCD sum rules, Adv. High Energy Phys. **2015**, 1 (2015).
[50] L. J. Reinders, H. Rubinstein, and S. Yazaki, Hadron properties from QCD sum rules, Phys. Rep. **127**, 1 (1985).
[51] S. Mallik, Operator product expansion at finite temperature, Phys. Lett. B **416**, 373 (1998).
[52] P. Gubler and D. Satow, Recent progress in QCD condensate evaluations and sum rules, Prog. Part. Nucl. Phys. **106**, 1 (2019).
[53] V. M. Belyaev and B. L. Ioffe, Determination of the baryon mass and baryon resonances from the quantum-chromodynamics sum rule. Strange baryons, Sov. Phys. JETP **57**, 716 (1983).
[54] H. G. Dosch, M. Jamin, and S. Narison, Baryon masses and flavour symmetry breaking of chiral condensates, Phys. Lett. B **220**, 251 (1989).
[55] B. L. Ioffe, QCD (Quantum chromodynamics) at low energies, Prog. Part. Nucl. Phys. **56**, 232 (2006).
[56] A. Bazavov *et al.*, Equation of state in $(2 + 1)$-flavor QCD, Phys. Rev. D, **90**, 094503 (2014).

[57] S. Borsanyi, Z. Fodor, C. Hoelbling, S. D. Katz, S. Krieg, and K. K. Szabó, Full result for the QCD equation of state with $(2 + 1)$ flavors, Phys. Lett. B **730**, 99 (2014).

[58] O. Kaczmarek, F. Karsch, F. Zantow, and P. Petreczky, Static quark-antiquark free energy and the running coupling at finite temperature, Phys. Rev. D **70**, 074505 (2004).

[59] K. Morita and S. H. Lee, Critical behavior of charmonia across the phase transition: A QCD sum rule approach, Phys. Rev. C **77**, 064904 (2008).